Diffeomorphic matching of distributions: A new approach for unlabelled point-sets and sub-manifolds matching

Joan Glaunes
LAGA
Université Paris 13
Villetaneuse, FRANCE

Alain Trouvé
CMLA
ENS de Cachan
Cachan, FRANCE

Laurent Younes
CIS
Johns Hopkins University
Baltimore, Md 21218

Abstract

In the paper, we study the problem of optimal matching of two generalized functions (distributions) via a diffeomorphic transformation of the ambient space. In the particular case of discrete distributions (weighted sums of Dirac measures), we provide a new algorithm to compare two arbitrary unlabelled sets of points, and show that it behaves properly in limit of continuous distributions on sub-manifolds. As a consequence, the algorithm may apply to various matching problems, such as curve or surface matching (via a sub-sampling), or mixings of landmark and curve data. As the solution forbids high energy solutions, it is also robust towards addition of noise and the technique can be used for nonlinear projection of datasets. We present 2D and 3D experiments.

1. Introduction

Matching embedded geometric structures is of particular importance in many computer vision tasks and medical imaging problems. The setting generally includes two images or volumes, within which points, curves or surfaces have been extracted, and formulates the following problems:

1. Detect suitable correspondences between the manifolds extracted from the first image and those extracted from the second.
2. Interpolate these correspondences to obtain a dense displacement field between the two images.

In most of the approaches developped for matching (like [3, 4, 14, 10, 1, 8, 13, 5]), the considered geometric structures are points and both problems are solved separately: the second is addressed by elastic matching techniques coupled with spline interpolation, and the first one (point to point correspondence) is most of the time solved by hand (labels being provided by experts), in the absence of a reliable matching procedure. As an exception, [16] addresses the problems simultaneously, with the paradigm that the best correspondences should correspond to the smoothest deformations, yielding an automated point matching procedure. To match higher dimensional structures (curves and surfaces), the same approach is used, after discretization and representation by a set of points.

However, curve and surface matching cannot be considered as limit problems of point matching (through discretization), because a given point in the discretized first manifold should be matched to some point of the second manifold, but not necessarily belonging to the set of points into which this manifold has been discretized. Our argument in this paper is that all these problems (surface, curve and unlabeled point matching) all are particular instances of a more general class of problems, which is matching measures on $\mathbb{R}^2$ or $\mathbb{R}^3$, and more generally distributions on these sets (ie. generalized functions). For this purpose, we develop a theory based on the action of diffeomorphisms on distributions (which we present here in the specific case of measures), along the lines of Grenander's deformable templates theory ([12]), and in the large-deformation setting, as developed in [17, 9, 15, 2, 11].

A significant contribution related to unlabeled point matching has been provided with the Robust Point Matching algorithm (RPM) [6] and further refinements with the Joint Clustering and Matching Algorithm (JCM) [7]. There, the approach essentially consists in estimating and matching two probability distributions, modeled as mixtures of Gaussians, with the assumptions that the second one is obtained from the first one by the action of an unknown deformation field on its centers, and that the two unlabeled point sets are random samples of these distributions. Such an approach, however, does not incorporate the important constraint that the estimated deformation is smooth and invertible. Moreover, the consistency issue is not addressed, and very hard to assert: this corresponds to the limit behavior of the algorithm in the case when the centers of the mixtures of Gaussian are them-

Proceedings of the 2004 IEEE Computer Society Conference on Computer Vision and Pattern Recognition (CVPR'04)
1063-6919/04 $20.00 © 2004 **IEEE**

selves obtained by discretizing two curves or surfaces, and the limit is taken with respect to the discretization accuracy. This is a fundamental issue, which essentially decides of the numerical reliability of the matching algorithm.

2. Mathematical Setup

2.1. Large deformation framework

This section provides the required component of the "large deformation framework" for diffeomorphic matching. In this setting, the starting object is a Hilbert space V, with norm $|\ |_V$, of smooth vector fields (at least C^1) defined on the background space $\mathbb{R}^d$. This space induces a sub-group $\mathcal{G}_V$ of diffeomorphisms as follows: to any time-dependent vector field $\mathbf{v} : t \to \mathbf{v}_t$, is associated the flow equation

$$\partial_t \phi_t = \mathbf{v}_t \circ \phi_t,\ \phi_0(x) = x\,, \tag{1}$$

which has a unique solution starting at $\phi_0 = \mathrm{id}$ when $t \mapsto |v_t|_V$ is integrable and under suitable regularity conditions on the elements of V ([9]). Then $\mathcal{G}_V$, defined by $\mathcal{G}_V = \{\ \phi_1^{\mathbf{v}} \mid |\mathbf{v}_t|_V \in L^1\ \}$, is a group, which can be equipped with a natural right-invariant geodesic distance $d(\phi, \phi') = \inf\{\int_0^1 |\mathbf{v}_t|_V dt \mid \phi_1^{\mathbf{v}} \circ \phi = \phi'\}$.

2.2. Group action on measures

Consider the set $\mathcal{M}_s$ of all signed measures (difference of two finite positive measures) on $\mathbb{R}^d$. The group $\mathcal{G}_V$ acts on $\mathcal{M}_s$ according to the action $(\phi, \mu) \to \phi\mu$ with

$$\phi\mu(f) = \int f \circ \phi\, d\mu \tag{2}$$

for any bounded measurable function f. In the case of a discrete measure $\mu = \sum_i \alpha_i \delta_{x_i}$ (where δ_x is the Dirac mass at location x), we have $\phi\mu = \sum_i \alpha_i \delta_{\phi(x_i)}$. The problem of matching two signed measures μ and ν will be formulated as finding $\hat{\phi} \in \mathcal{G}_V$ as close as possible to the identity mapping (for the distance d on $\mathcal{G}_V$) such that $\hat{\phi}\mu$ is close to ν, for some metric between measures, both constraints being represented by penalty terms in a variational problem. To specify the metric which is used to compare $\hat{\phi}\mu$ and ν, we introduce a second Hilbert space $\mathcal{I}$, with norm $|\ |_I$, containing continuous, bounded *functions* on $\mathbb{R}^d$, with the constraint

$$|f|_\infty \leq c|f|_I \tag{3}$$

for a given c. Let I^* be the space of continuous linear forms on I. Assumption (3) implies that integration with respect to signed measure, which is a continuous linear form on bounded continuous functions is also continuous for the Hilbert structure on I, so that $\mathcal{M}_s$ can also be considered as a subset of I^*. The distance between two signed measures μ and μ' is now taken as $|\mu - \mu'|_{I^*}$, with the usual definition: $|\nu|_{I^*} = \sup(\int f d\mu, f \in I, |f|_I = 1)$.

This norm can be computed as follows. The Riesz representation theorem implies that, for all $y \in \mathbb{R}^d$, there exists an element, $K_I\delta_y$ of I such that, for all $f \in I$, $f(y) = \int f d\delta_y = \langle K_I\delta_y, f\rangle_I$. This implies that, for all $\mu \in \mathcal{M}_s$,

$$\int f(y)d\mu(y) = \int \langle K_I\delta_y, f\rangle_I d\mu(y) = \Big\langle \int K_I\delta_y d\mu(y), f\Big\rangle_I$$

In particular, denoting $K_I\mu = \int K_I\delta_y d\mu(y)$, and taking the supremum of both sides over all f with $|f|_I = 1$, we have

$$|\mu|_{I^*}^2 = |K_I\mu|_I^2 = \int K_I\mu(x)d\mu(x)$$

which finally yields, denoting $k_I(y, x) = (K_I\delta_y)(x)$

$$|\mu|_{I^*}^2 = \int k_I(x, y)d\mu(x)d\mu(y) \tag{4}$$

If $\mu = \sum_i c_i\delta_{x_i}$ is a weighted sum of Dirac measures, this yields

$$|\mu|_{I^*}^2 = \sum_{i,j} c_i c_j k_I(x_i, x_j)$$

which is particularly simple when k_I is given.

2.3. Variational formulation

We define the optimal matching, $\hat{\phi}$ between two signed measures μ and ν as a minimizer of $J_{\mu,\nu}(\phi) \doteq d(Id, \phi)^2 + |\phi\mu - \nu|_{I^*}^2/\sigma_R^2$, σ_R^2 being a trade-off parameter. Introducing the kinetic energy $\int_0^1 |\mathbf{v}_t|_V^2 dt$, we get equivalently that $\hat{\phi} = \phi_1^{\hat{\mathbf{v}}}$ (cf (1)) where $\hat{\mathbf{v}}$ is a minimizer of

$$J_{\mu,\nu}(\mathbf{v}) = \int_0^1 |\mathbf{v}_t|_V^2 dt + \frac{1}{\sigma_R^2}|\phi_1^{\mathbf{v}}\mu - \nu|_{I^*}^2 \tag{5}$$

An attractive aspect of this variational formulation is its ability to handle point sets matching problems for which μ and ν are two positive discrete measures and the limit problem of matching continuous distributions supported by submanifolds.

2.4. Existence and consistency results

In this subsection we state, without proofs, two important properties of this variational formulation. The first one is an existence theorem, which is true under suitable regularity conditions on V.

Theorem 1 (Existence) *For given μ, ν in $\mathcal{M}_s$ there exists a minimizing solution $\hat{\mathbf{v}}$ of (5).*

The second one is the consistency property mentionned in the introduction, still valid under suitable regularity conditions on V.

Theorem 2 (Consistency) *Let μ and ν be two* probability distributions on $\mathbb{R}^d$ *and let $x_1, \cdots, x_m$ and $y_1, \cdots, y_n$ be iid samples drawn from distributions μ and ν. Let $\hat{\mu}_m = \frac{1}{m}\sum_i \delta_{x_i}$ and $\hat{\nu}_n = \frac{1}{n}\sum_j \delta_{y_j}$ be the associated empirical measures. Then if $\hat{\phi}(m,n)$ is a minimizer of $J_{\hat{\mu}_m,\hat{\nu}_n}$, almost surely, $\hat{\phi}(m,n)$ tends uniformly (up to the extraction of a subsequence) to $\hat{\phi}$, minimizer of $J_{\mu,\nu}$, when $m,n \to \infty$.*

3. Derivation of the algorithm

3.1. Gradient computation for general measures

Our estimation of the optimal matching between two distributions μ and ν is based on the implementation of a gradient algorithm for

$$J(\mathbf{v}) = \int_0^1 |\mathbf{v}_t|_V^2 dt + \frac{1}{\sigma_R^2}|\phi_1^{\mathbf{v}}\mu - \nu|_{I^*}^2$$

in $L^2([0,1],V)$, the Hilbert space of time-dependent elements of V with square integrable norms.

We compute the variations of J with respect to a variation $\mathbf{v}_h = \mathbf{v} + h\widetilde{\mathbf{v}}$. For a given quantity A, we denote $\widetilde{A}$ the variation of A with respect to h, i.e. the derivative of A_h at $h=0$.

Since the variation of the first term is straightforward, we focus on the second term $\mathcal{E} = |\phi_1^{\mathbf{v}}\mu - \nu|_{I^*}^2$. We have

$$\widetilde{\mathcal{E}} = 2\langle \widetilde{\phi_1^{\mathbf{v}}\mu}, \phi_1^{\mathbf{v}}\mu - \nu\rangle_{I^*}$$

Let $K_I : I^* \to I$ be the canonical isometry between I and its dual space I^* generated by the Riesz representation theorem i.e. for any $\nu \in I^*$ and $g \in I$, $\nu(g) = \langle K_I\nu, g\rangle_I = \langle \nu, K_I^{-1}g\rangle_{I^*}$. This operator has already been introduced, as applied to measures, in section 2.1. Let $f_1 = K_I(\phi_1^{\mathbf{v}}\mu - \nu) \in I$. Since $\widetilde{\phi_1^{\mathbf{v}}\mu} \in I^*$, we can write

$$\widetilde{\mathcal{E}} = 2\widetilde{\phi_1^{\mathbf{v}}\mu}(f_1) = \mu(\widetilde{f_1 \circ \phi_1^{\mathbf{v}}}) = \mu(d_{\phi_1^{\mathbf{v}}}f_1.\widetilde{\phi_1^{\mathbf{v}}}).$$

Now, denoting $\phi_{st}^{\mathbf{v}} = \phi_t^{\mathbf{v}} \circ (\phi_s^{\mathbf{v}})^{-1}$, the variation of the deformation map $\phi_1^{\mathbf{v}}$ satisfies [2],

$$\widetilde{\phi_1^{\mathbf{v}}} = \int_0^1 d_{\phi_t^{\mathbf{v}}}\phi_{t1}^{\mathbf{v}}.\widetilde{\mathbf{v}}_t \circ \phi_t^{\mathbf{v}} dt.$$

Therefore,

$$d_{\phi_1^{\mathbf{v}}}f_1.\widetilde{\phi_1^{\mathbf{v}}} = \int_0^1 (d(f_1 \circ \phi_{t1}^{\mathbf{v}}).\widetilde{\mathbf{v}}_t) \circ \phi_t^{\mathbf{v}} dt,$$

and thus

$$\begin{aligned}\widetilde{\mathcal{E}} &= \int_0^1 \phi_t^{\mathbf{v}}\mu(d(f_1 \circ \phi_{t1}^{\mathbf{v}}).\widetilde{\mathbf{v}}_t)dt \\ &= \int_0^1 \left(\int_{\mathbb{R}^d} d_x(f_1 \circ \phi_{t1}^{\mathbf{v}}).\widetilde{\mathbf{v}}_t(x) d(\phi_t^{\mathbf{v}}\mu)\right) dt \\ &= \int_0^1 \left(\int_{\mathbb{R}^d} \langle \nabla_x(f_1 \circ \phi_{t1}^{\mathbf{v}}), \widetilde{\mathbf{v}}_t(x)\rangle d(\phi_t^{\mathbf{v}}\mu)\right) dt.\end{aligned}$$

The linear form

$$\phi_t^{\mathbf{v}}\mu\nabla(f_1 \circ \phi_{t1}^{\mathbf{v}}) : \mathbf{u} \mapsto \int_{\mathbb{R}^d} \langle \nabla_x(f_1 \circ \phi_{t1}^{\mathbf{v}}), \mathbf{u}_t(x)\rangle d(\phi_t^{\mathbf{v}}\mu)$$

is continuous on V and therefore belongs to V^*. Introducing, as above, the operator $K_V : V^* \to V$ inducing the canonical isometry, we find

$$\widetilde{\mathcal{E}} = \int_0^1 \langle K_V(\phi_t^{\mathbf{v}}\mu\nabla(f_1 \circ \phi_{t1}^{\mathbf{v}})), \widetilde{\mathbf{v}}_t\rangle_V dt,$$

and the gradient of J in $L^2([0,1],V)$ writes

$$(\nabla J)_t(x) = 2\mathbf{v}_t(x) + \frac{2}{\sigma_R^2}K_V(\phi_t^{\mathbf{v}}\mu\nabla(K_I(\phi_1^{\mathbf{v}}\mu - \nu) \circ \phi_{t1}^{\mathbf{v}})). \quad (6)$$

3.2. Application to Dirac measures

When measures μ and ν are weighted sums of Dirac measures, $\mu = \sum_{i=1}^m a_i\delta_{x_i}$ and $\nu = \sum_{i=1}^n b_i\delta_{y_i}$, the formula for J and its gradient can be rewritten to provide an explicit formulation of the variational problem. We use the notation $x_i(t) = \phi_t^v(x_i)$ and

$$\phi_1^{\mathbf{v}}\mu - \nu = \sum_{i=1}^m a_i\delta_{x_i(t)} - \sum_{i=1}^n b_i\delta_{y_i} = \sum_{i=1}^{n_z} c_i\delta_{z_i}.$$

First, the error term of J writes

$$\mathcal{E} = |\phi_1^{\mathbf{v}}\mu - \nu|_{I^*}^2 = \sum_{i,j=1}^{n_z} c_i c_j k_I(z_i, z_j).$$

Now we use the following remark : when trajectories $x_i(t)$ are fixed, the vector fields of lowest energy take the form

$$\mathbf{v}_t(x) = \sum_{i=1}^m k_V(x_i(t), x)\alpha_i(t),$$

where $k_V(x,y)$ is the kernel operator corresponding to space V, which satisfies $\beta^* k_V(x,y)\alpha = \langle k_V(x,\cdot)\alpha, k_V(y,\cdot)\beta\rangle_V$. This is a general fact for landmark matching methods [13, 5].

Thus, the variables of our minimization problem become the vectors $\alpha_i(t)$ and the functional J rewrites

$$\begin{aligned}J &= \int_0^1 \left(\sum_{i,j=1}^m \alpha_j(t)^* k_V(x_i(t), x_j(t))\alpha_i(t)\right. \\ &\qquad \left. + \frac{1}{\sigma_R^2}\sum_{i,j=1}^{n_z} c_i c_j k_I(z_i, z_j)\right) dt.\end{aligned}$$

Next we compute the explicit formulation of the gradient to be implemented in the matching code. We have

$$\begin{aligned} f_1(x) &= K_I(\phi_1^{\mathbf{v}}\mu - \nu)(x) = \sum_{i=1}^{n_z} c_i k_I(z_i, x), \\ f_1 \circ \phi_{t1}^{\mathbf{v}}(x) &= \sum_{i=1}^{n_z} c_i k_I(z_i, \phi_{t1}^{\mathbf{v}}(x)), \\ \nabla(f_1 \circ \phi_{t1}^{\mathbf{v}})(x) &= \sum_{i=1}^{n_z} c_i (d_x \phi_{t1}^{\mathbf{v}})^* . \nabla_2 k_I(z_i, \phi_{t1}^{\mathbf{v}}(x)). \end{aligned}$$

Moreover, $\phi_t^{\mathbf{v}}\mu = \sum_{i=1}^m a_i \delta_{x_i(t)}$, so if we denote by δ_x^α the element of V^* such that $\delta_x^\alpha(\mathbf{u}) = \langle \mathbf{u}(x), \alpha \rangle$, we have

$$\phi_t^{\mathbf{v}}\mu\nabla(f_1 \circ \phi_{t1}^{\mathbf{v}}) = \sum_{j=1}^m a_j \delta_{x_j(t)}^{\beta_j(t)},$$

with $\beta_j(t) = (d_{x_j(t)}\phi_{t1}^{\mathbf{v}})^* . \beta_j(1)$ and

$$\beta_j(1) = \sum_{i=1}^{n_z} c_i \nabla_2 k_I(z_i, \phi_1^{\mathbf{v}}(x_j)). \tag{7}$$

The gradient expression is

$$(\nabla J)_t(x) = 2\sum_{j=1}^m k_V(x_j(t), x)(\alpha_j(t) + \beta_j(t)/\sigma_R^2).$$

The quantity $\beta_j(t)$ can be computed by numerical integration, since we have :

$$\begin{aligned} d_{x_j(t)}\phi_{t1}^{\mathbf{v}} &= d_{x_j}\phi_1^{\mathbf{v}} . (d_{x_j}\phi_t^{\mathbf{v}})^{-1}, \\ \partial_t (d_{x_j}\phi_t^{\mathbf{v}})^{-1} &= -(d_{x_j}\phi_t^{\mathbf{v}})^{-1} . d_{x_j(t)}\mathbf{v}_t, \\ \partial_t d_{x_j(t)}\phi_{t1}^{\mathbf{v}} &= -d_{x_j(t)}\phi_{t1}^{\mathbf{v}} . d_{x_j(t)}\mathbf{v}_t, \end{aligned}$$

and eventually,

$$\partial_t \beta_j(t) = (\partial_t d_{x_j(t)}\phi_{t1}^{\mathbf{v}})^* . \beta_j(1) = -(d_{x_j(t)}\mathbf{v}_t)^* . \beta_j(t). \tag{8}$$

Now since $\mathbf{v}_t = \sum_{k=1}^m k_V(x_k(t), \cdot)\alpha_k(t)$, we have

$$d_{x_j(t)}\mathbf{v}_t = \sum_{k=1}^{n_x} \partial_2 k_V(x_k(t), x_j(t))\alpha_k(t).$$

4. Experiments

5. Experiments

This section presents simulations processed on synthetic examples with a MATLAB implementation of a gradient descent on the functional J, as given by formula 7. We have used kernels k_V and k_I defined on $\Omega = \mathbb{R}^2$ and such that

$$k_V(x, y) = f_V\left(\frac{|x-y|^2}{\sigma_V^2}\right) Id$$

$$k_I(x, y) = f_I\left(\frac{|x-y|^2}{\sigma_I^2}\right),$$

i.e. k_V and k_I are isotropic, translation and rotation invariant. For functions f_V and f_I wa have tried $f_V(u) = f_I(u) = \exp(-u)$ (gaussian kernels) and $f_V(u) = f_I(u) = \frac{1}{1+u}$. This second choice gives the best results and has been selected for the simulations.

The main steps of the gradient descent algorithm are

- Initialisation
  Set initial trajectories $x_i(t) = x_i$ and $\alpha_i(t) = 0$
- Iteration loop : $(x, \alpha) \rightarrow (\hat{x}, \hat{\alpha})$.
  - Compute $\beta_j(1)$ with formula 7.
  - Compute $\beta_j(t)$ by integrating equation 8.
  - Set $\alpha_i(t) \leftarrow \alpha_i(t) - \lambda(2\alpha_i(t) + \beta_i(t))$ where λ is the gradient step.
  - Compute new trajectories $\hat{x}_i(t)$ by integrating

$$\partial_t \hat{x}_i(t) = \sum_{i=1}^m k_V(x_j(t), \hat{x}_i(t))\alpha_j(t).$$

  - Compute new vectors $\hat{\alpha}_i(t)$ by inverting the linear systems

$$\partial_t \hat{x}_i(t) = \sum_{i=1}^m k_V(\hat{x}_j(t), \hat{x}_i(t))\hat{\alpha}_j(t).$$

The two last steps are actually needed to ensure that during minimization, trajectories $x_i(t)$ are kept equal to $\phi_t^{\mathbf{v}}(x_i)$, where $\mathbf{v}$ is computed from $\alpha_i(t)$.

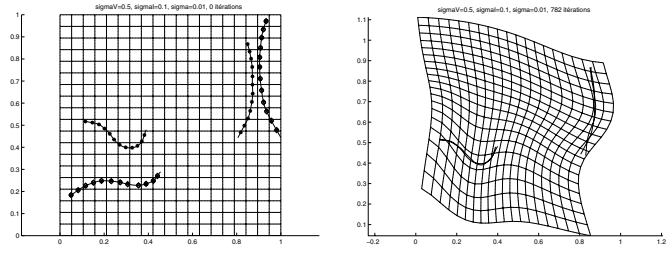

Figure 1. Matching with two pairs curves (see text for details).

Figure 1 shows the result of matching two pairs of smapled curves. Initial landmark points (lowest and rightmost curves) are drawn as diamonds and targets as stars. Note that these are the only information given to the algorithm for the minimization process. In particular, the algorithm does not "know" that there are two curves. On the right frame (final state) are drawn the target curve and the

deformation of the whole initial curve which superimpose almost exactly.

Figure 1 shows the result of a matching process between two pairs of curves given by their sampling. Initial landmark points are drawn as diamonds and targets as stars. Note that these are the only information given to the algorithm for the minimization process. In particular, the algorithm do not ”know” that there are two curves. On the right frame (final state) are drawn the target curve and the deformation of the whole initial curve.

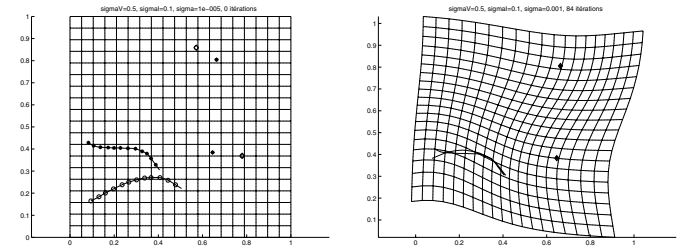

Figure 2. Experiment with one curve and two landmarks (see text for details).

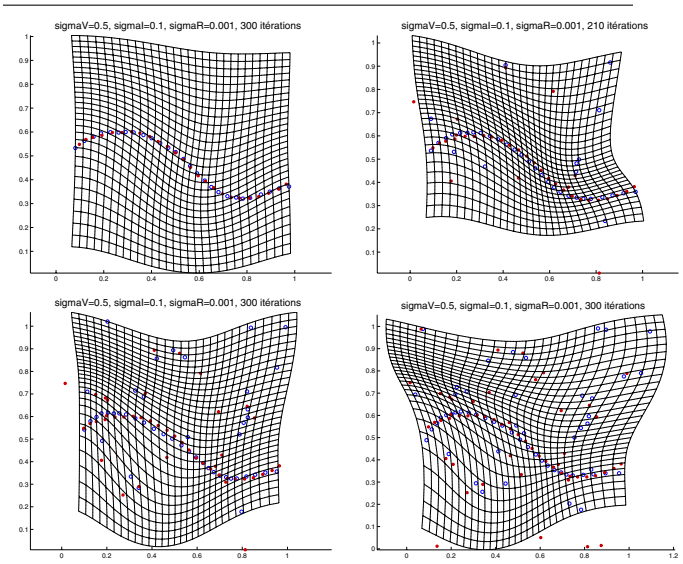

Figure 3. Robustness against outliers (0, 20, 40 and 60 outlier points added)

Experiment 2 illustrates the possibility to perform a matching with both of landmark and curve data. For the simulation we have assigned a weight of $1/3$ for each of the 2 landmarks **and** the curve, which means each of the 12 sample points of the curve has weight $1/36$; thus equal importance is given to the three items.

Experiment 3 explores the robustness of the algorithm against the presence of outliers. It shows how the deformation varies when more and more random points are added both to the initial and target datasets. The conclusion is that, while the global deformation may be affected by the noise, its effect on the initial curve remains essentially constant.

Next (figures 3,4,5,6) we have processed a series of experiments of matching a circle to a deformed closed curve. The only curve which is drawn is the image of the initial circle under the current deformation map (The initial circle is locates on the lower-left part of the grid).

In figure 4 we sample the curves at various rates and process the algorithm with the same parameters. When sampling rates are equal, the algorithm matches exactly pairs of landmarks. The interesting case comes with different sampling rates : in this case the deformed data fits along the target curve without matching specifically any of its landmarks. This illustrates the consistency of the algorithm, as explained in the section 2.4.

In figure 5 a gaussian noise is added to the positions of the target landmarks, with increasing variance. The deformed curve remains remarkably stable, finding an aver-

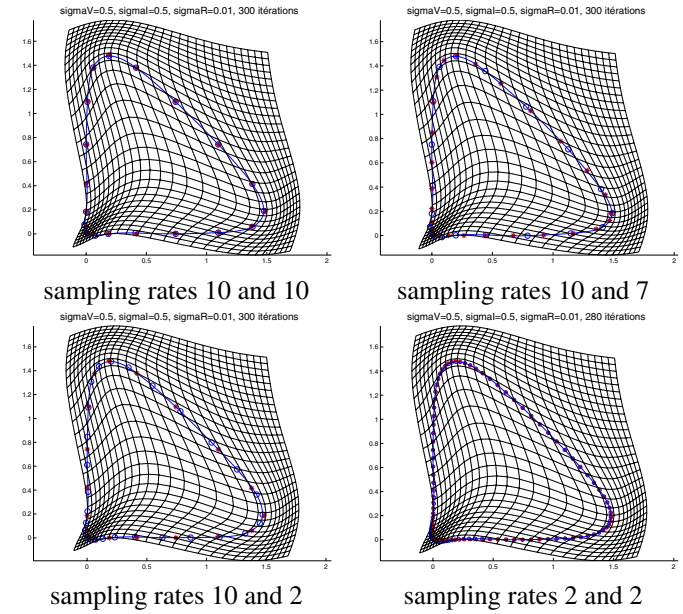

Figure 4. Comparing different sampling rates.

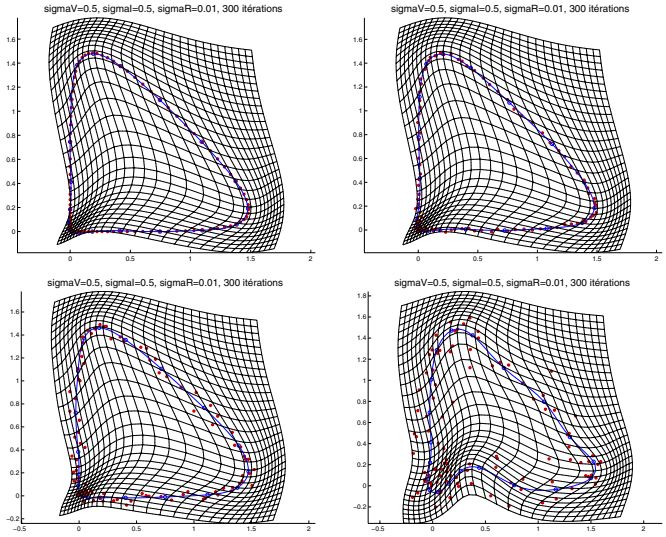

Figure 5. Analyzing the effect of noisy data (variances of noise are 0, 0.01, 0.03, and 0.1)

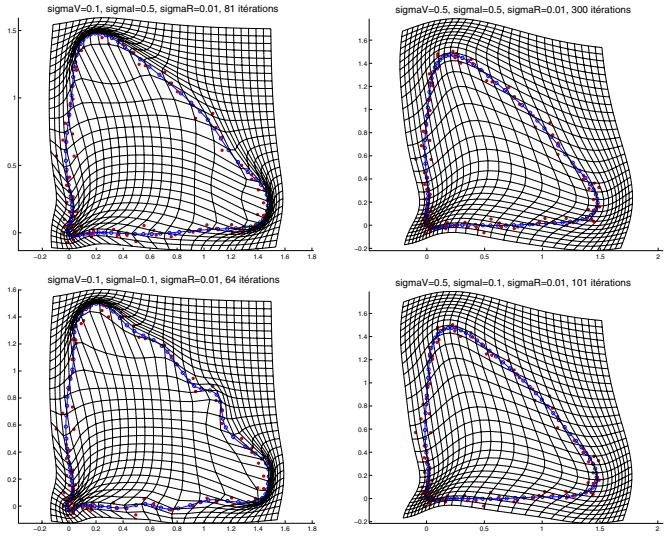

Figure 6. Testing different kernel sizes on noisy data.

age position within the target points, even for significantly large noise.

In figure 6 we vary the parameters σ_V and σ_I and process a noisy data sample (the third one in figure 5). When these parameters decrease, the deformation map becomes more sensitive to local variations of the data.

In figure 7, the matching algorithm was processed on A. Rangarajan's dataset, available on his website. In the fish experiment, data needed to be translated on the x-axis before processing to produce good results (our method does not yet implement affine registration).

6. Conclusion

The algorithm introduced in this work present several interesting features. Mathematically, it has the advantage to imbed the problem of submanifold matching in a general framework, measure matching, in which convergence and consistency results express naturally. On a more practical level, we model both deformations fields and measures as linear sums of kernels functions which sizes can be adjusted to work at a given spatial scale. The synthetic experiments allowed us to demonstrate several good properties, such as robustness against noise and outliers, or against different resamplings of the curves. Since the first redaction of this report, experiments on brain 3D data have been started, with promising results. A preliminar example is provided in figure 8.

References

[1] N. Arad, N. Dyn, D. Reisfeld, and Y. Yeshurun, *Image warping by radial basis functions: application to facial expressions*, CVGIP: Graphical Models and Image Processing, 56 (1994), pp. 161–172.

[2] M. F. Beg, M. I. Miller, A. Trouvé, and L. Younes, *Computing large deformation metric mappings via geodesics flows of diffeomorphisms*, Int. J. Comp. Vis (to appear), (2003).

[3] F. L. Bookstein, *The measurement of Biological Shape and Shape Change*, vol. 24 of Lecture Notes in Biomathematics, Springer–Verlag, Berlin, 1978.

[4] L. Bookstein, F, *Morphometric tools for landmark data; geometry and biology*, Cambridge University press, 1991.

[5] V. Camion and L. Younes, *Geodesic interpolating splines*, in EMMCVPR 2001, M. Figueiredo, J. Zerubia, and K. Jain, A, eds., vol. 2134 of Lecture notes in computer sciences, Springer, 2001.

[6] H. Chui and A. Rangarajan, *A new point matching algorithm for non-rigid registration*, Computer Vision and Understanding, 89 (2003), pp. 114–141.

[7] H. Chui, L. Win, R. Schultz, J. Duncan, and A. Rangarajan, *A unified non-rigid feature registration method for brain mapping*, Medical Image Analysis, 7 (2003), pp. 113–130.

[8] T. Cootes, C. Taylor, D. Cooper, and J. Graham, *Active shape models: their training and application*, Comp. Vis. and Image Understanding, 61 (1995), pp. 38–59.

[9] P. Dupuis, U. Grenander, and M. Miller, *Variational problems on flows of diffeomorphisms for image matching*, Quaterly of Applied Math., (1998).

[10] N. Dyn, *Interpolation and approximation by radial and related functions*, in Approximation theory VI: vol. 1, K. Chui,

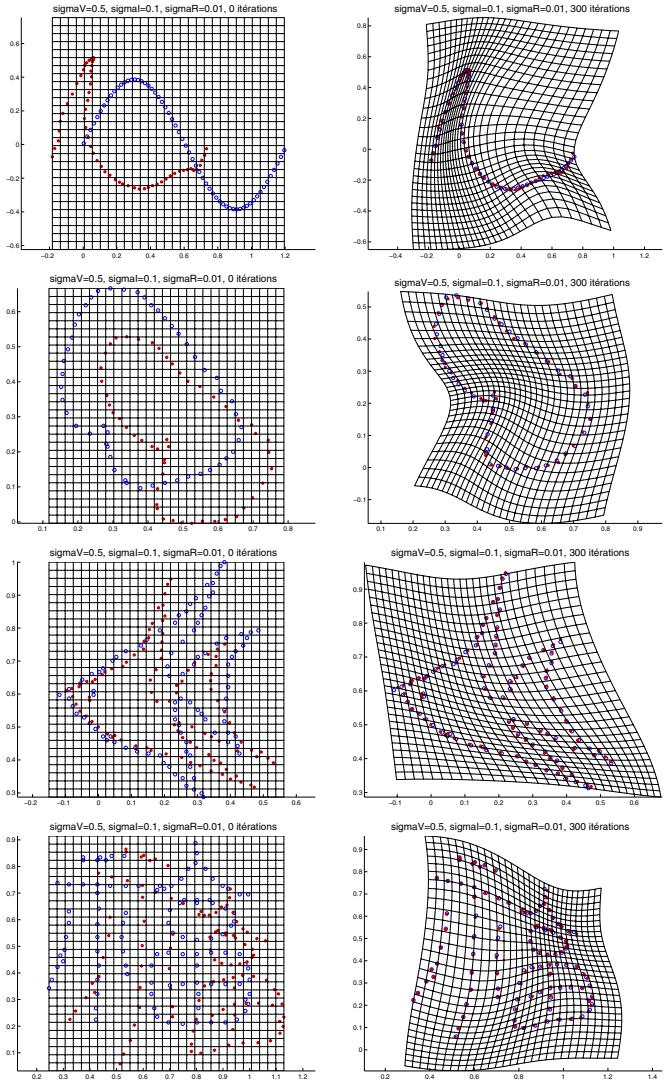

Figure 7. A. Rangarajan's data set

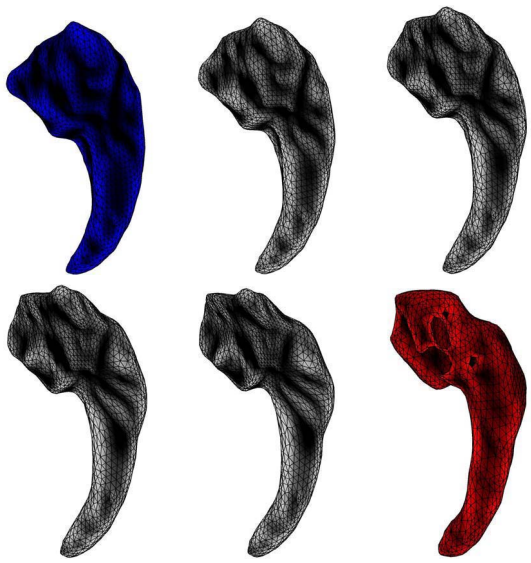

Figure 8. Experiment in 3D with hippocampus cortical surfaces. Deformations are estimated after sampliing the surface of the initial and the target Hippocampi. The four intermediate views provide the effect of the time-dependent deformation process induced by (1).

C, L. Shumaker, L, and D. Ward, J, eds., Academic Press, 1989, pp. 211–234.

[11] J. Glaunès, M. Vaillant, and I. Miller, M, *Landmark matching via large deformation diffeomorphisms on the sphere*, Journal of Mathematical Imaging and Vision, MIA 2002 special issue, (2003).

[12] U. Grenander and I. Miller, M, *Computational anatomy: An emerging discipline*, Quarterly of Applied Mathematics, LVI (1998), pp. 617–694.

[13] S. Joshi and M. Miller, *Landmark matching via large deformation diffeomorphisms*, IEEE transactions in image processing, 9 (2000), pp. 1357–1370.

[14] D. G. Kendall, *Shape manifolds, procrustean metrics and complex projective spaces*, Bull. London Math. Soc., 16 (1984), pp. 81–121.

[15] I. Miller, M and L. Younes, *Group action, diffeomorphism and matching: a general framework*, Int. J. Comp. Vis, 41 (2001), pp. 61–84. (*Originally published in electronic form in: Proceeding of SCTV 99, http://www.cis.ohio-state.edu/ szhu/SCTV99.html*).

[16] A. Rangarajan, E. Mjolsness, S. Pappu, L. Davachi, S. Goldman-Rakic, P, , and S. Duncan, J, *A robust point matching algorithm for autoradiograph alignment*, in Visualization in Biomedical Computing (VBC), H. Hohne, K and R. Kikinis, eds., 1996, pp. 277–286.

[17] A. Trouvé, *Diffeomorphism groups and pattern matching in image analysis*, Int. J. of Comp. Vis., 28 (1998), pp. 213–221.